

Article

Sustainable Design of a Tiny House: Using a Life Cycle Assessment Approach to Compare the Environmental Performance of Industrial and Earth-Based Building Systems

Letizia Dipasquale ^{1,*} , Giada Giuffrida ^{2,*} , Natalia Jorquera Silva ^{3,4}, Riccardo Maria Pulselli ⁵ and Rosa Caponetto ² 

¹ Department of Architecture, University of Florence, 50121 Firenze, Italy

² Department of Civil Engineering and Architecture, University of Catania, 95124 Catania, Italy

³ Department of Architecture, Faculty of Engineering, University of La Serena, La Serena 1700000, Chile

⁴ Department of Architecture, Faculty of Architecture and Urbanism, University of Chile, Santiago 8330111, Chile

⁵ Heritage–Architecture–Urbanism Department, Mediterranean University of Reggio Calabria, 89124 Reggio Calabria, Italy

* Correspondence: letizia.dipasquale@unifi.it (L.D.); giada.giuffrida@unict.it (G.G.)

Abstract: The increased concerns about climate change, diminishing natural resources, and environmental degradation call for deep research into new environmentally friendly building systems that use natural or recycled materials. The article presents an assessment of the environmental and climatic benefits associated with the construction of a tiny house made of *quincha*, a building system based on a wooden structure filled with locally sourced earth and straw. The tiny house is located in the Elqui Valley, in the Chilean region of Coquimbo, and it is designed to be compact, functional, comfortable, and efficient. The study uses a life cycle approach to assess the environmental impacts of building construction, maintenance, and end-of-life treatment, comparing the adopted *quincha* solution with four hypothetical scenarios using industrial, prefabricated, and/or synthetic construction materials currently adopted in the region. The thermal performance of all the analyzed solutions is also included in order to provide insights into the impact of the operational phase. This paper demonstrates that the *quincha* solution, in the face of lower thermal insulation compared to the other prefabricated solutions (the U-value of the *quincha* wall is 0.79 W/m²K while the U-value of the best prefabricated wall is 0.26 W/m²K), has higher thermal inertia (time lag (TL) and decrement factor (DF) are, respectively, 6.97 h and 0.60, while other systems have a TL below 4 h and DF higher than 0.81). For a quantitative environmental evaluation, the carbon footprint (global warming potential), water footprint, and embodied energy indicators are assessed through LCA, which takes into account the mass of the materials and their emission factors. The effectiveness of the *quincha* solution is also reflected in environmental terms; in fact, it is found to have the lowest carbon footprint (2635.47 kgCO₂eq) and embodied energy (42.7 GJ) and the second-lowest water footprint (2303.7 m³). Moreover, carbon sequestration values, which are assessed by estimating the carbon contained in building systems using wood and straw, demonstrate that the *quincha* tiny house is the only solution that can theoretically reach carbon neutrality (with its carbon storage value at −5670.21 kgCO₂eq).

Keywords: raw earth materials; bio-based materials; sustainable construction technology; sustainable design; wattle and daub



Academic Editor: Bo-Tao Huang

Received: 11 December 2024

Revised: 24 January 2025

Accepted: 30 January 2025

Published: 5 February 2025

Citation: Dipasquale, L.; Giuffrida, G.; Jorquera Silva, N.; Pulselli, R.M.; Caponetto, R. Sustainable Design of a Tiny House: Using a Life Cycle Assessment Approach to Compare the Environmental Performance of Industrial and Earth-Based Building Systems. *Buildings* **2025**, *15*, 491. <https://doi.org/10.3390/buildings15030491>

Copyright: © 2025 by the authors. Licensee MDPI, Basel, Switzerland.

This article is an open access article distributed under the terms and conditions of the Creative Commons Attribution (CC BY) license (<https://creativecommons.org/licenses/by/4.0/>).

1. Introduction

In response to the escalating concerns about climate change, diminishing natural resources, and widespread environmental degradation, the construction industry is increasingly turning its focus toward sustainable building systems that aim to significantly reduce their environmental footprint [1]. The growing awareness of the urgent need for responsible building practices is reshaping how we think about the entire life cycle of construction, from resource extraction to eventual demolition or repurposing. Sustainable construction systems should be designed with the primary objective of not only reducing waste and carbon emissions but also preserving the delicate balance of ecosystems for future generations [2,3].

The choices made regarding construction methods, materials, and energy sources play a pivotal role in determining a building's overall environmental impact [4]. From a sustainability perspective, these decisions should be grounded in a thorough and clear understanding of their ecological consequences, aiming to provide shelter, comfort, and utility without depleting Earth's resources.

Given the pressing need to develop an informed and forward-thinking approach to the built environment, with a strong focus on minimizing environmental impacts, Life Cycle Assessment (LCA) is increasingly recognized as a crucial tool in the Architectural, Engineering, and Construction (AEC) industries [5]. LCA is a systemic approach that provides a comprehensive framework for evaluating the environmental footprint of building materials, systems, and processes throughout their entire life cycle, from extraction and manufacturing to use and eventual disposal or recycling. This enables stakeholders to compare alternatives, make more sustainable decisions across all stages of construction, and adopt strategies that minimize environmental harm, fostering more sustainable construction practices [6,7]. In addition to LCA, thermal performance is another critical factor in assessing the sustainability of buildings. A building's thermal performance significantly influences its energy consumption and capacity to maintain comfortable indoor environments while minimizing environmental harm [8]. High thermal performance means reduced energy demands for heating and cooling, which directly contributes to lower greenhouse gas emissions and overall environmental impact [9].

This study evaluates the environmental impact and analyzes the thermal performance of a tiny house constructed using a modern reinterpretation of the traditional Chilean *quincha* technique, a variation on the wattle and daub construction method [10–12]. The traditional *quincha* building technique consists of a wooden framework filled with light earth, which is a mixture of clayey earth and plant fibers in varying proportions. This mixture can be applied either dry or wet, depending on the moisture content and the condition of the materials. The primary structural framework, typically made from logs, reeds, or sawn timber, forms the building's main support. A secondary framework, intended to contain the mixture of straw and earth and support the outer cladding, can be made from branches, laths, or wires arranged in various configurations [13]. This method offers numerous environmental advantages, such as reduced embodied energy and the use of renewable, biodegradable materials. The *quincha* technique also improves the thermal performance of the building by leveraging the natural insulation properties of earth and straw mixes, helping to regulate indoor temperatures and reduce the need for artificial heating or cooling. This passive approach to thermal regulation is especially beneficial in regions like the Elqui Valley, where temperature fluctuations are significant: during summer, the outdoor temperature minimum is 15 °C and the maximum 30 °C, while during winter the outdoor temperature minimum is 10 °C and the maximum 16 °C [14]. The analyzed tiny house was built in the Coquimbo region of Chile, with locally available natural materials, such as earth, stone, and straw, sourced primarily from the surrounding area. A portion

of the soil used in the mix was repurposed from earth blocks (adobes) salvaged from abandoned ruins, giving these materials a renewed purpose while minimizing the need for newly extracted resources.

Recent studies have highlighted that tiny houses significantly reduce energy consumption, material use, and greenhouse gas emissions, when compared to single-family houses or apartments [15–23]. Crawford and Stephan [15] demonstrated that tiny houses could reduce per capita greenhouse gas (GHG) emissions by 70% over their lifetime compared to conventional houses, taking into account both embodied and operational emissions. Kuittinen et al. [23] examined the environmental benefits of tiny wooden houses, focusing on material use, land efficiency, energy consumption, and total emissions. Typically, tiny houses show superior performance on a per-building or per-capita basis. However, when the impact is assessed on a per-unit-area basis, they perform less favorably than conventional buildings. All studies show that the operational emissions of tiny houses depend significantly on their energy consumption, which varies significantly with climatic conditions [20–23]. Only a few authors separate embodied impacts from operational ones, favoring further comparisons [24,25].

Moreover, several studies in recent years have demonstrated the benefits of using earth as a building material, particularly in reducing environmental impacts and enhancing the thermo-hygrometric performance of buildings. However, many of these studies are confined to comparisons of individual building components, such as plaster and vertical walls [26–34].

This study highlights the pivotal role of material choices and construction systems in shaping the overall environmental impact of a tiny house. Indeed, the analysis herein includes a comparison of the environmental impact and thermal performance of the tiny house with four other hypothetical scenarios that use systems commonly employed in the construction of new houses in rural areas in Chile. By comparing these solutions, we can demonstrate the environmental effects of material and technique choices in the construction of new buildings. Additionally, an analysis of the thermal performance of all the considered solutions is carried out, which is crucial for understanding their energy efficiency [20].

By examining both the environmental and thermal performance of the tiny house, this study underscores the potential of traditional construction techniques, like *quincha*, to offer viable and sustainable alternatives to contemporary building methods. The use of locally sourced and recycled materials not only reduces the environmental impact but also supports local economies and fosters a deeper connection to the natural and cultural landscape. This project highlights the importance of integrating vernacular knowledge with modern sustainability practices to create buildings that are both ecologically responsible and culturally relevant [35].

Furthermore, this study contributes to the growing body of research on sustainable architecture by providing a detailed case study of how traditional techniques can be adapted and applied in modern contexts. As global construction practices increasingly focus on reducing carbon footprints and promoting sustainability, the lightweight *quincha* method serves as a model for how ancient building practices can be harnessed to meet contemporary environmental challenges. Through this analysis, the research advocates for a more localized, resource-efficient approach to construction that aligns with the principles of environmental stewardship and long-term sustainability.

2. Materials and Methods

2.1. Case Study Description

The territorial context of the tiny house is the Chilean “Norte Chico”, a semi-arid area considered an environmental transition zone between the Atacama Desert and the fertile

central Chilean valley, where earth-based construction has traditionally been practiced. The Elqui Valley runs from west to east through the Coquimbo region and is flanked by the Andes Mountains to the east and the Pacific Ocean to the west (Figure 1). The area's climate is characterized by hot summers and mild winters, with scarce rainfall concentrated in the winter months. This region suffers from critical water scarcity, which, combined with climate change, results in a systematic decrease in winter rainfall and an increase in annual thermal oscillation. The Coquimbo region is situated in a seismically active zone due to its position along the boundary of the Nazca and South American tectonic plates. This region, like much of Chile, is part of the Pacific Ring of Fire, known for frequent and powerful seismic activity. Coquimbo has experienced numerous significant earthquakes, including the 8.3 magnitude event in 2015, which triggered a tsunami and caused widespread damage [36].



Figure 1. Landscape of the Elqui Valley, the location of the case study.

The analyzed case study is a tiny house with a footprint of 28 m², designed specifically for occasional vacation use (Figure 2). The building design adapts to the natural space between two pre-existing trees, which were preserved to protect the valuable vegetation in this semi-arid environment.

The floor plan of the building consists of two main rooms. The first, located at the entrance, contains the living room and kitchen. The second is the bedroom, with a bathroom situated between the two rooms. All spaces feature windows, and natural ventilation is optimized through strategically placed openings on opposite sides. The building's orientation runs east to west, with the primary openings positioned on the western façade (Figure 3).



Figure 2. Tiny house analyzed as a case study, shown in its surrounding context.

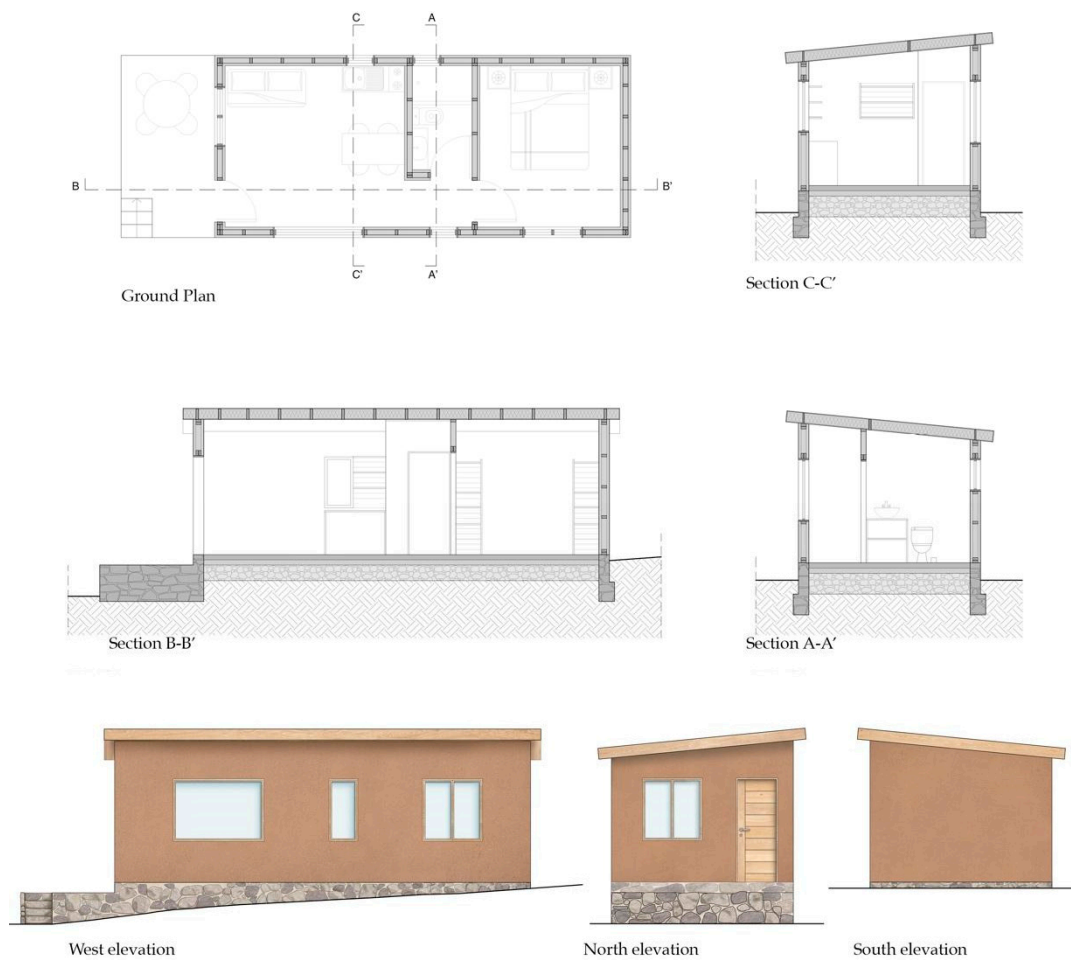


Figure 3. Plans and sections of the analyzed tiny house.

The building is constructed using the *quincha alivianada* technique [13], a modern adaptation of the traditional Chilean method known as *quincha*. This method uses a wooden

framework filled with materials of varying densities, depending on local availability and the site's specific climatic conditions, and typically features an earthen plaster. *Quincha* is a localized variant of the widespread wattle and daub technique, employed in many regions worldwide and adapted to local resources and contexts. The technique involves weaving a lattice of wooden or bamboo laths ("wattle") and filling it with a mixture of earth and straw or other plant fibers ("daub"). In the specific case of the tiny house analyzed, the technique was implemented with an emphasis on utilizing locally sourced materials, skills, and labor as much as possible, promoting sustainability from environmental, economic, and social perspectives. At the same time, the goal was to create a high-performance structure in terms of thermal efficiency, mechanical strength, and earthquake resistance.

The stratigraphy of the *quincha* wall in the case study consists of a structural grid constructed from squared timber elements, an infill composed of a mixture of earth and straw, and a protective lime-stabilized earthen plaster coating.

Stones sourced from the site are used to build a stone masonry foundation. These stones are set in place using lime mortar, which provides both strength and breathability for the foundation. A thin layer of cement was applied to finish the floor surface. The primary structural framework is constructed using radiata pine wood. Vertical and horizontal wooden beams measuring 5×10 cm are installed to form the skeleton of the building. A secondary structure composed of diagonal elements, measuring 2.5×5 cm, supports and encloses the wall infill, which is made of clay-rich earth in a plastic state and abundant wheat straw fibers (Figure 4). The earthen mix is prepared by combining local soil with abundant wheat straw fibers. The soil was primarily sourced from the surrounding area near the construction site, with 20% of the mix composed of reclaimed adobe bricks salvaged from abandoned sites. This mix, while plastic (in a malleable state), was used as wall infill. Earth and straw are compacted between wooden supports to form walls, with straw fibers reducing weight and enhancing thermal insulation.



Figure 4. Building section and construction step where the wooden framework is manually filled with light earth.

As already said, the walls are finished with a 3 cm thick earthen plaster, incorporating 10% lime in the mixture to improve durability and resistance to weathering.

The roof is composed of wooden beams insulated with straw-lightened earth, supported by an OSB panel, and sealed with an asphalt waterproof membrane.

Once the walls and roof are completed, the interior is finished, including final touches on the earthen plaster, and furniture.

The entire construction process took four months, carried out by a team of four local workers (two bricklayers and two carpenters). The main furniture pieces were handcrafted on-site from pine wood.

2.2. Construction Systems Used for Comparison

The *quincha* construction system was compared with other common systems used in new house construction in the rural context in Chile. In recent years, prefabricated houses in Chile have gained popularity due to the growing need for quick and affordable housing solutions. The prefabricated construction industry has seen notable growth, with several companies emerging, offering modern and customized designs tailored to specific client needs [37]. Figure 5 illustrates the wall stratigraphy of the case study tiny house (Q) alongside four comparative wall systems, labeled W1, W2, LSF, and CPS.

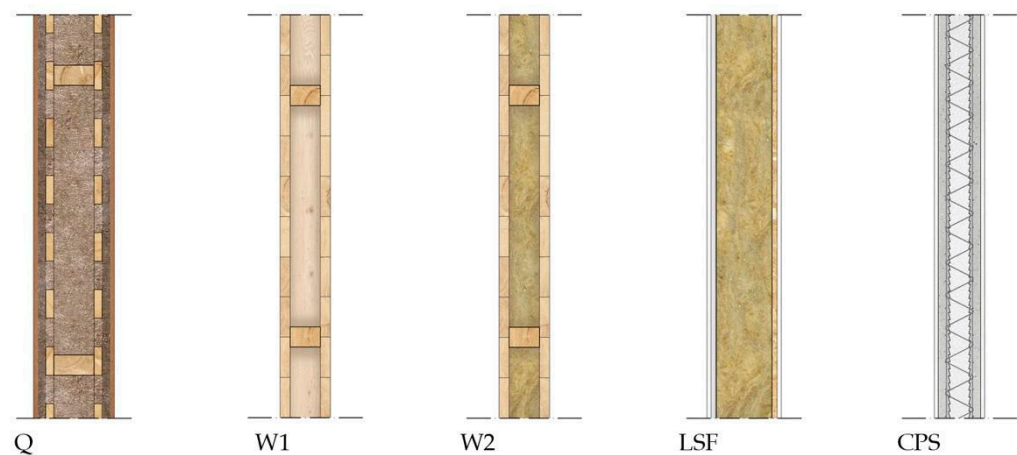


Figure 5. Stratigraphy of the construction systems used for comparison.

2.2.1. Wooden Prefabricated House System (W1 and W2)

One of the prevalent construction systems for new buildings in rural and suburban areas in Chile involves prefabricated wooden structures, with or without thermal insulation, installed on-site over concrete foundations. The system primarily utilizes pine (*Pino radiata*), an abundant, fast-growing resource, along with native woods like *Lenga* and *Raulí*, particularly in southern regions where hardwood is more available.

Wooden components, such as wall panels, floor joists, and roof trusses, are prefabricated in a factory and then assembled on-site. The system typically features structural wooden frames with 5×7.5 cm studs, glass wool insulation, and wooden board cladding. However, insulation is not always used in the building enclosure, often resulting in a poor thermal performance. Other insulation materials like glass wool, polystyrene, or mineral wool can be integrated into the panels to enhance thermal efficiency. The total wall thickness ranges from 10 to 12 cm.

After prefabrication, components are transported to the site and assembled on the concrete slab foundations.

Once the structural frame is erected, insulation—if included—is installed, followed by external cladding materials such as wood siding, fiber cement boards, or metal sheeting,

chosen based on durability and aesthetic preferences. Interior finishes, such as drywall, plaster, or wood paneling, are then applied to complete the internal structure. The roofs are typically covered with trapezoidal or corrugated metal sheets, providing enhanced protection against weather conditions.

The wall W1 that was compared to the *quincha* case study has a timber frame made of 5×7.5 cm elements, with 10 cm wide and 2.5 cm thick closing boards. The foundation is made of reinforced concrete, with a concrete floor. The roof uses the same structural system as the walls and is externally covered with a trapezoidal metal sheet. The W2 variant shares the same structure as W1 but includes glass wool insulation.

2.2.2. Light Steel Frame Prefabricated System (LSF)

The Light Steel Frame Prefabricated System is a widely used prefabricated construction method in Chile that involves the use of cold-formed galvanized steel, typically in C-sections or U-sections, to create the structural framework for walls, floors, and roofs [38]. The panels are composed of equidistant steel profiles, spaced between 400 and 600 mm, with top and bottom elements. Thermal insulation materials such as mineral wool, polyurethane foam, or glass wool are integrated into the steel frame to enhance energy efficiency. The system supports various cladding materials, such as fiber cement, gypsum board, or OSB paneling. The steel profiles are cut, shaped, and pre-drilled in the factory. Once on-site, they are assembled into the structural framework, including wall studs, floor joists, and roof trusses. After the frame is erected, insulation is installed between the steel members, followed by the application of external cladding. Interior finishes, such as gypsum board or other finishings, are then applied to complete the building. The LSF wall analyzed consists of a framework using 14×4 cm U-shaped steel profiles, insulated with glass wool. It is internally clad with a gypsum board and externally with an OSB panel. Both the interior and exterior are finished with cement plaster.

2.2.3. Concrete Panel System with EPS Insulation (CPS)

The last system analyzed, the Concrete Panel System, consists of an expanded polystyrene (EPS) core enclosed between two layers of galvanized wire mesh embedded in a concrete mortar for structural reinforcement [39]. Widely adopted in recent years for low- to middle-income housing projects in Chile and rural construction, it is also used for extensions or modifications to existing structures. The EPS core provides insulation, while the galvanized wire mesh, made of steel wire coated with zinc to prevent corrosion, ensures structural integrity and seismic resistance. After installation, the panels are coated with shotcrete or cement plaster, bonding to the mesh to create a solid, load-bearing surface.

The panels are prefabricated in a factory, produced in standard sizes, and transported to the site for quick assembly. Their lightweight nature makes installation fast and efficient, reducing labor and construction time compared to traditional methods. Once placed on the foundation, the final layer of shotcrete or cement is applied, completing the structural system.

2.3. Thermal Performance Assessment of Enclosure Components

The following paragraph focuses on the thermal properties of the materials which compose the analyzed technologies. Data concerning conventional building materials, such as wood elements and glass wool insulation, were taken from the ISO 10456:2007 [40]. Raw earth render thermal properties were taken from a previous work by the authors [41].

The production of the earth mixes used to build the *quincha* wall is very artisanal and somewhat variable [13]. For that reason, in this study, we wanted to investigate how much the composition of the material that composes the *quincha* wall alters the final expected thermal performance.

To quantify the thermal performance of the *quincha* enclosure components, a parametric study was performed based on the results of a previously published literature review [42] and the work by Volhard [43] and Wieser et al. [44]. In detail, the relation found between the bulk density, thermal conductivity, and specific heat capacity of lightened earthen materials was used to hypothesize the thermal performance of the *quincha* components. Figure 6 plots the bulk density of the lightened earthen mix against the expected thermal conductivity and the specific heat capacity values, based on Volhard's study [43]. As stated in Volhard's work [43], bulk densities from 200 kg/m³ to 1200 kg/m³ are typical for light earth mixes, while bulk density values from 1300 kg/m³ to 1600 kg/m³ are more typical for straw–clay materials.

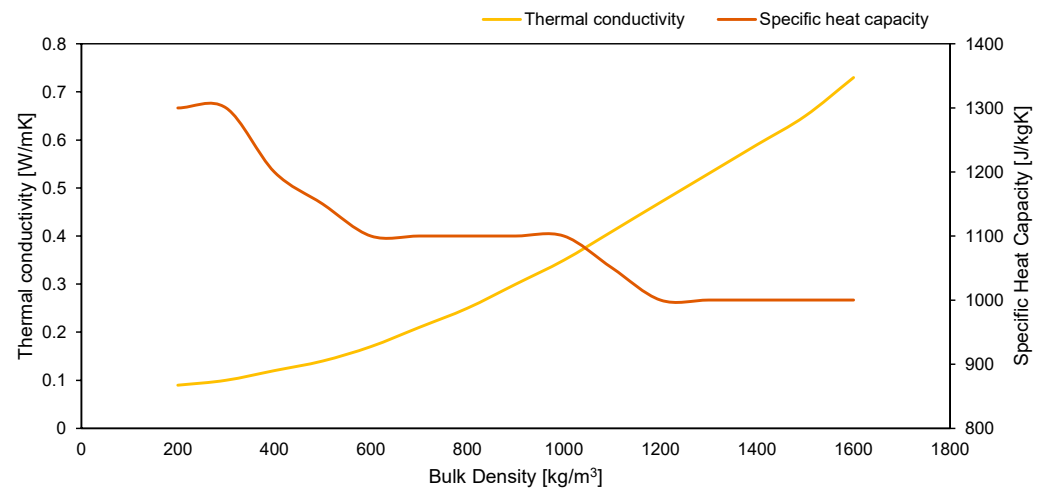


Figure 6. Variability of thermal conductivity and specific heat capacity of earthen materials for *quincha*, depending on density (Data from ref. [43]).

In the following, to verify how much the earth mix density changes the thermal performance of the *quincha* wall and roof enclosure elements, we analyze two extreme cases: the Q500 case, where an earth mix density of 500 kg/m³ is assumed, and the Q1500 case, where an earth mix density of 1500 kg/m³ is considered. In particular, for the Q500 case, a thermal conductivity of 0.14 W/mK and a specific heat capacity of 1150 J/kgK are estimated; meanwhile, for the Q1500 case, a thermal conductivity of 0.65 W/mK and a specific heat capacity of 1000 J/kgK are predicted [42].

The construction and material properties of all the examined materials making up the enclosure elements (walls, roofs, foundations) are reported in Table 1.

Table 1. Enclosure construction and thermal properties of the analyzed assemblies.

Abbr.	Layer	t_{tot}	t	λ	c_p	ρ
		[m]	[m]	[W/mK]	[J/kgK]	[kg/m ³]
Foundations						
W1, W2, LSF, CPS Q	Concrete footing	0.400	0.400	1.60	1000	2300
	Stone footing	0.400	0.400	1.50	900	2750
Walls						
Q500	Raw earth render		0.030	0.62	800	1939
	Light earth	0.200	0.140	0.14	1150	500
	Raw earth render		0.030	0.62	800	1939

Table 1. Cont.

Abbr.	Layer	t_{tot}	t	λ	c_p	ρ
		[m]	[m]	[W/mK]	[J/kgK]	[kg/m ³]
Q1500	Raw earth render	0.200	0.030	0.62	800	1939
	Straw clay		0.140	0.65	1000	1500
	Raw earth render		0.030	0.62	800	1939
W1	Wood cladding	0.125	0.025	0.12	2700	450
	Air gap		0.075	-	-	-
	Wood cladding		0.025	0.12	2700	450
W2	Wood cladding	0.125	0.025	0.12	2700	450
	Glass wool		0.075	0.04	850	105
	Wood cladding		0.025	0.12	2700	450
LSF	Cement plaster	0.184	0.010	0.90	1000	1800
	Plasterboard		0.012	0.25	1000	900
	Glass wool		0.140	0.04	850	105
	OSB panel		0.012	0.13	1600	530
	Cement plaster		0.010	0.90	1000	1800
CPS	Cement plaster	0.125	0.010	0.90	1000	1800
	Cement mortar		0.025	1.40	1000	2000
	EPS panel		0.055	0.036	1480	35
	Cement mortar		0.025	1.40	1000	2000
	Cement plaster		0.010	0.90	1000	1800
Roofs						
Q500	Wooden plank	0.214	0.012	0.13	1600	500
	Light earth		0.150	0.14	1150	500
	OSB panel		0.012	0.13	1600	530
	Bituminous membrane		0.040	0.17	1700	1250
Q1500	Wooden plank	0.214	0.012	0.13	1600	500
	Straw-clay		0.150	0.65	1000	1500
	OSB panel		0.012	0.13	1600	530
	Bituminous membrane		0.040	0.17	1700	1250
W1	Wooden plank	0.032	0.025	0.13	1600	500
	Corrugated metal sheet		0.007	50.00	450	7800
W2	Wooden plank	0.197	0.025	0.13	1600	500
	Glass wool panel		0.140	0.04	850	105
	Wooden plank		0.025	0.13	1600	500
	Corrugated metal sheet		0.007	50.00	450	7800
LSF	Cement plaster	0.181	0.010	0.90	1000	1800
	Plasterboard		0.012	0.25	1000	900
	Glass wool panel		0.140	0.04	850	105
	OSB panel		0.012	0.13	1600	530
	Corrugated metal sheet		0.007	50.00	450	7800
CPS	Cement plaster	0.122	0.010	0.90	1000	1800
	Cement mortar		0.025	1.40	1000	2000
	EPS panel		0.055	0.036	1480	35
	Cement mortar		0.025	1.40	1000	2000
	Corrugated metal sheet		0.007	50.00	450	7800

The assessment of the thermal performance of the enclosures' construction (*Quincha*, Uninsulated and Insulated Prefabricated Wood, Light Steel Frame and Concrete Panel

Systems) was carried out using steady-state parameters, such as the U-value and surface mass, based on the ISO 13786:2017 [45].

The U-value expresses the expected rate of heat transfer through building components, which should be kept low to limit heat dispersion. At the same time, it is also important to provide a certain thermal mass to the enclosure elements, in order to favor heat wave damping and delay; for this reason, the wall's surface mass value should be sufficiently high (in general, above 230 kg/m²) [41,46]. Surface mass can be easily calculated by multiplying the thickness of the layer by its density. The periodic thermal transmittance (Y_{ie}) is defined as the complex amplitude of the density of the heat flow rate through one surface of the component or assembly, divided by the complex amplitude of the temperature on that side when the temperature adjacent to the other side is held constant [45,47]. An optimal building component should have a low periodic thermal transmittance to reduce the impact of the outside thermal load. The time lag is an expression of the time delay between the outdoor and the indoor temperature peaks; an acceptable time lag should be greater than six hours, while the optimal performance is expected when the time lag is greater than twelve hours. Finally, the decrement factor expresses the reduction in the heat flux entering from the outdoor surface of the building enclosure and that reaching the indoor surface of the building enclosure; a sufficient decrement factor value should be lower than 0.60, while optimal performances are expected when it is lower than 0.15.

2.4. Life Cycle Assessment at the Building Scale

To assess the carbon footprint and mitigation potential of this construction, and to compare it with the environmental impact of other construction systems commonly used for similar projects in Chile, a Life Cycle Assessment (LCA) approach is used. This method allows for quantifying the impact on the resource consumption, emissions, and overall sustainability of the building, considering all stages from material extraction to the end of its useful life.

As defined by ISO 14040-14044 [48,49], Life Cycle Assessment (LCA) involves the collection and evaluation of a system's inputs, outputs, and potential environmental impacts throughout its entire life cycle. The functional unit defined for this study is the total volume of the tiny house, with system boundaries extending across all major life cycle processes, thus covering the entire "cradle to grave" span of the building. The analysis evaluates the impact of critical materials and energy consumption across the following life cycle phases:

- Upstream: the production of materials and construction components, starting from raw material extraction.
- Transportation: the delivery of raw materials and construction elements to the building site.
- Core: the construction phase of the tiny house.
- Maintenance: material replacements over time, based on the estimated lifespan of key building components.
- End of Life: the disassembly, transport, disposal, or treatment of waste materials at the building's end of life.

Figure 7 illustrates the life cycle phases, highlighting the sequence of processes along with their respective inputs and outputs, including emissions to air, water, and soil. A service life of 100 years is assumed for the tiny houses, allowing for an estimation of the maintenance impact due to the periodic replacement of components subject to wear and tear. The inventory data are based on the volumes and masses of materials used for each wall. Note that while two different assumptions of soil mixtures for the *quincha* wall

and roof were used to compare thermal performance, the LCA analysis is based on the quantities of materials actually used on the building site.

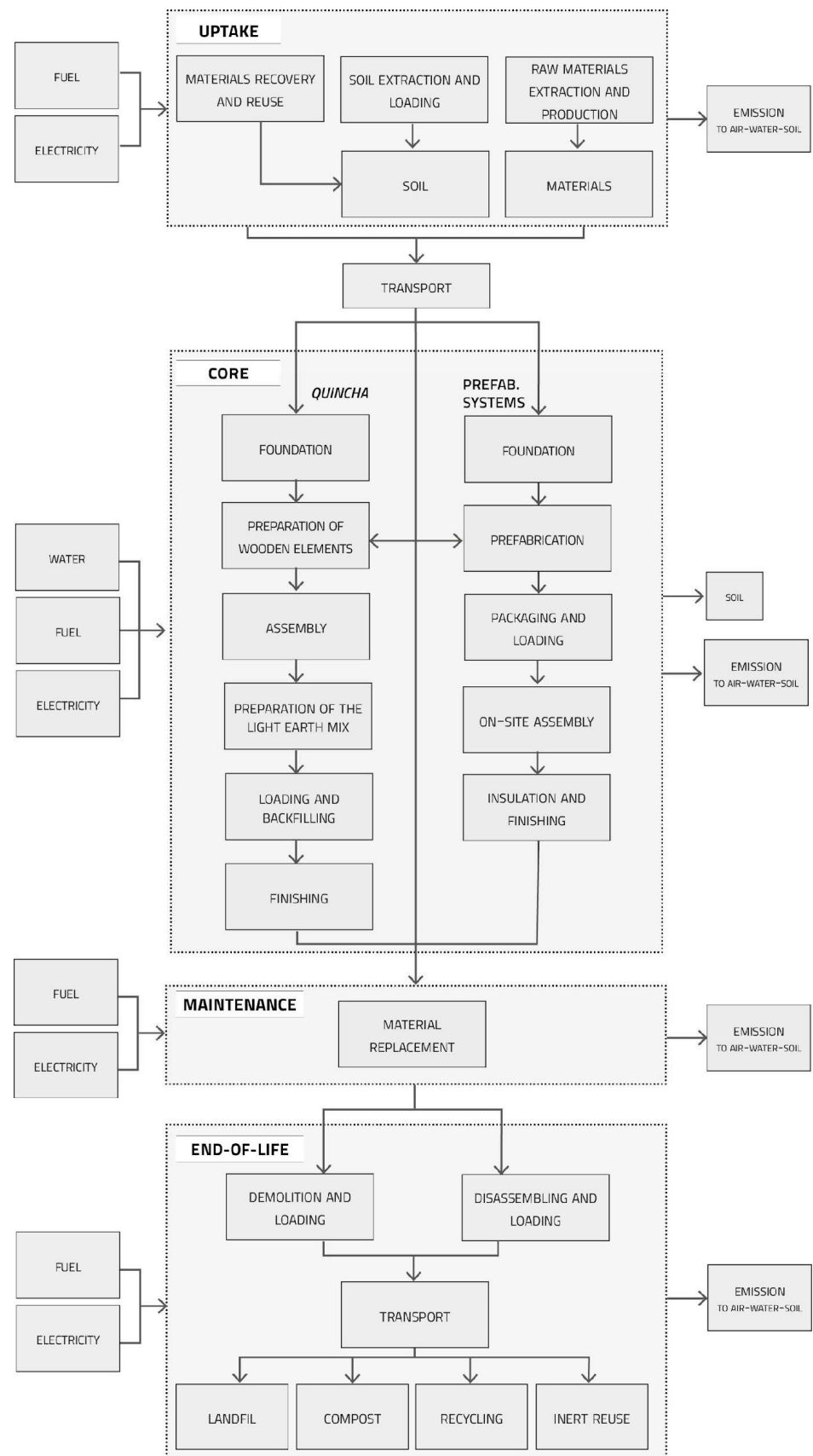


Figure 7. Life Cycle Analysis flow diagram (Credit: R. Pulselli, L. Dipasquale).

Emissions from transporting construction materials and components by truck were calculated based on the materials' points of origin. For example, the stone was sourced directly from the excavation site where the house is located. Approximately 80% of the earth used was extracted from a nearby source, within a 5 km radius of the site, while the remaining 20% was obtained by repurposing adobe blocks salvaged from a nearby demolition, further reducing transport-related emissions. The straw was locally sourced, while a distance of 500 km was estimated for the wood, which was obtained from southern Chile, where it is produced.

The life cycle inventory data (see Table 2) were sourced from direct interviews with housebuilders and homeowners and a literature review [26–34,41]. The life cycle inventory (LCI) data represent the detailed accounting of all inputs and outputs for a product system across its life cycle. This includes the quantification of raw materials, energy consumption, and other environmental exchanges associated with each process. These data form the foundation for evaluating the environmental impacts of the different construction systems analyzed.

Table 2. Life cycle inventory of the analyzed systems.

Phase	Inputs	Unit	Q	W1	W2	LSF	CPS
		mq	28.00	28.00	28.00	28.00	28.00
UPSTREAM: Raw materials	Foundation						
	Stone	kg	49,600.00	-	-	-	-
	Lime	kg	4364.80	-	-	-	-
	Cement mortar	kg	1820.00	-	-	-	-
	Sand	kg	7140.00	-	-	-	-
	Concrete	kg	-	12.14	12.14	12.14	12.14
	Walls						
	Wood	m ³	3.50	4.02	4.02	-	-
	Earth (soil)	kg	2500.00	-	-	-	-
	Straw	kg	300.00	-	-	-	-
	Linseed oil	kg	16.50	-	-	-	-
	Glass wool insulation	kg	-	-	93.90	181.05	-
	Lime	kg	196.43	-	-	-	-
	Plasterboard	kg	-	-	-	512.11	-
	Steel	kg	-	-	-	645.00	105.55
	OSB	m ³	-	-	-	0.78	-
	Cement plaster	kg	-	-	-	1681.2	5736.64
	EPS	kg	-	-	-	-	86.68
	Roof						
	Wood	m ³	0.83	1.40	1.40	-	-
	Earth (soil)	kg	625.00	-	-	-	-
	Straw	kg	300.00	-	-	-	-
	OSB	m ³	0.50	-	-	-	-
	Plasterboard	kg	-	-	-	266.11	-
	Plywood	kg	0.36	-	-	-	87.50
	Bituminous membrane	kg	133.60	-	-	-	-
	Glass wool insulation	kg	-	-	141.00	94.10	-
	Corrugated sheet metal	kg	-	1800.00	1800.00	1764.00	-
	Steel	kg	-	-	-	176.40	56.26
	Cement plaster	kg	-	-	-	436.80	3276.00
Concrete	kg	-	-	-	-	87.50	
EPS	kg	-	-	-	-	46.20	

Table 2. Cont.

Phase	Inputs	Unit	Q	W1	W2	LSF	CPS	
		m ^q	28.00	28.00	28.00	28.00	28.00	
Traveled distance								
Transport	From extraction to factory	t km	113.45	1045.83	1052.55	1098.03	1192.04	
	From supplier to factory	t km	-	1355.51	1355.51	-	1986.74	
	From extraction to building yard	t km	18.63	-	-	-	-	
	From factory to building yard	t km	1134.50	271.10	271.10	1252.21	397.00	
	From supplier to building yard	t km	1367.17	3215.00	3228.10	3660.10	3973.48	
	Return of machineries	t km	1.60	25.80	25.80	25.80	25.80	
Production in factory								
CORE: manufacturing	Cutting	m ³	5.42	5.42	15.65	-	-	
	Screwing	m ³	5.42	5.42	16.51	-	-	
	Loading	m ³	-	5.66	13.49	17.69	12.30	
	Construction on-site							
	Wooden cutting	m ³	4.32	-	-	-	-	
	Wooden screwing	m ³	4.32	-	-	8.10	-	
Earth mixing	m ³	9.71	-	-	1.29	-		
Maintenance (replaced covering materials)								
Maintenance	Earth cladding	m ³	0.80	-	-	-	-	
	Lime mortar	kg	225.00	-	-	-	-	
	Cement mortar	kg	728.00	-	-	-	3605.06	
	Bituminous membrane	kg	1202.40	-	-	-	-	
	Corrugated sheet metal	kg	-	1800.00	1800.00	1764.00	-	
	Wood paint	kg	-	77.11	96.39	-	-	
	Cement plaster	kg	-	-	-	12.85	-	
End-of-life treatment								
End-of-Life	Demolition and loading	m ³	27.42	12.14	12.14	12.14	24.44	
	Disassembling and loading	m ³	4.32	5.66	13.49	17.69	-	
	Transport to landfill	t km	6.68	90.00	101.75	313.05	1986.74	
	Transport to incineration plant	t km	-	-	-	-	-	
	Transport to composting plant	t km	186.25	135.55	135.50	-	-	
	Transport to inert landfill (direct reuse)	t km	3146.24	1334.96	1334.96	1517.00	1517.00	
	Transport to recycling	t km	1037.60	-	-	-	-	
	Landfill	kg	133.60	1800.00	2034.90	6261.04	9394.83	
	Incineration	kg	-	-	-	-	-	
	Compost	kg	3725.00	2711.03	2710.00	-	-	
	Inert landfill (direct reuse)	kg	13,324.80	26,699.20	30,340.00	30,340.00	30,340.00	

The emission factors (EFs) for the carbon footprint (global warming potential) were assessed using the CML-IA characterization method in SimaPro 9.0.0 (v2024), based on data from the Ecoinvent 3.6 database. The AWARE method was employed to assess the water footprint, while the Cumulative Energy Demand (CED) method was used to evaluate the embodied energy values.

3. Results and Discussion

3.1. Expected Thermal Performance

3.1.1. Foundations

As neither the stone nor the concrete footing solutions are insulated, their thermal performance is similarly poor. The U-values are $2.54 \text{ W/m}^2\text{K}$ for the concrete footing and $2.29 \text{ W/m}^2\text{K}$ for the stone footing, meaning that thermal dispersion to the ground could play a major role in the thermal behavior of the tiny house.

3.1.2. Walls

If we now consider the *quincha* wall (Q) and compare its expected thermal performances with the other wall constructs, we find the following results related to the U-value (Figure 8), surface mass (Figure 9), periodic thermal transmittance Y_{ie} (Figure 10), time lag (Figure 11), and decrement factor (Figure 12).

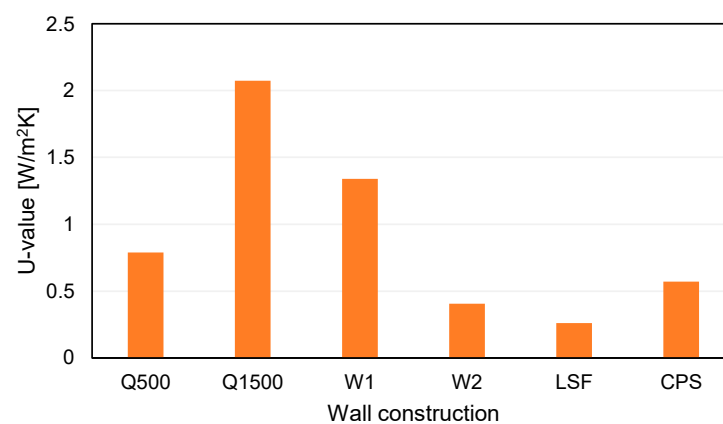


Figure 8. U-values of the investigated wall building systems.

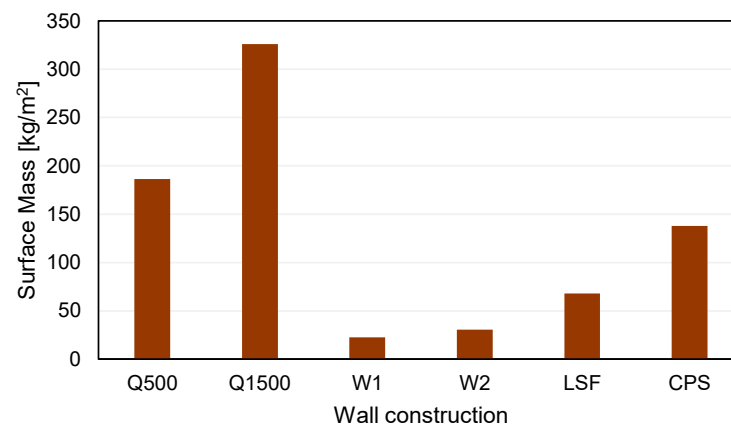


Figure 9. Surface masses of the investigated wall building systems.

Figure 8 shows the U-values of the analyzed wall solutions. The Light Steel Frame wall (LSF) has the lowest thermal transmittance ($0.26 \text{ W/m}^2\text{K}$), followed by the Insulated Prefabricated Wood solution (W2) ($0.41 \text{ W/m}^2\text{K}$) and the Concrete Panel System (CPS) ($0.57 \text{ W/m}^2\text{K}$). It is evident that, even if the *quincha* wall Q500 is built with a lightweight earth mix, its thermal transmittance remains quite high ($0.60 \text{ W/m}^2\text{K}$), due to the fact that the earth matrix is still very conductive. This fact is exacerbated when an earth mix density of 1500 kg/m^3 is considered, as demonstrated by the Q1500 U-value ($2.07 \text{ W/m}^2\text{K}$). The Uninsulated Prefabricated Wood solution (W1) has the highest U-value ($1.34 \text{ W/m}^2\text{K}$).

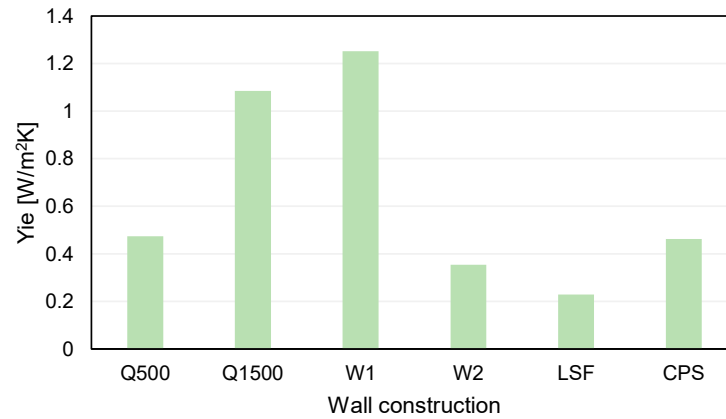


Figure 10. Periodic thermal transmittance of the investigated wall building systems.

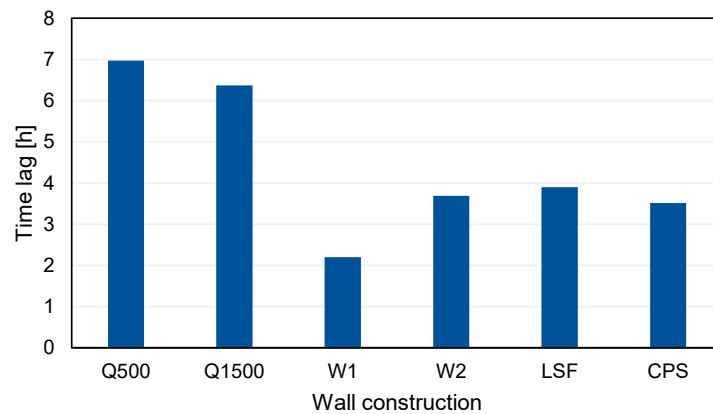


Figure 11. Time lags of the investigated wall building systems.

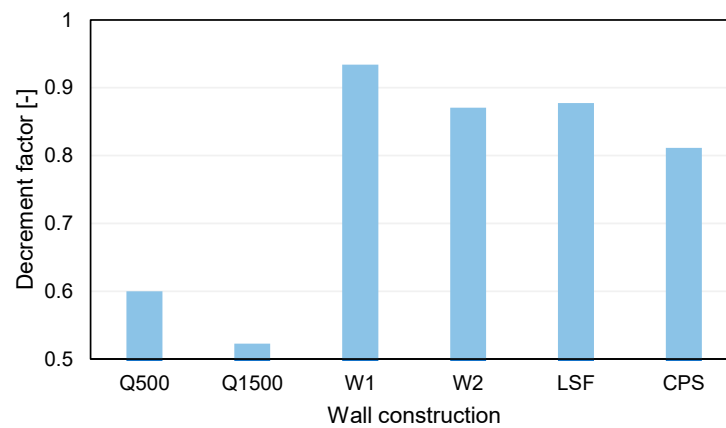


Figure 12. Decrement factors of the investigated wall building systems.

In Figure 9, the surface mass of the Q500 wall is 186 kg/m^2 , while the Q1500 mass is 326 kg/m^2 . These surface mass values are slightly higher than those of the W1 wall (23 kg/m^2) and W2 wall (30 kg/m^2). Moreover, the LSF solution has a surface mass of 68 kg/m^2 . Finally, the third-best surface mass value is that of the CPS wall, which is calculated as 138 kg/m^2 .

Figure 10 highlights the good dynamic thermal performance of the LSF, W2, and Q500 walls, with Y_{ie} values of $0.23 \text{ W/m}^2\text{K}$, $0.35 \text{ W/m}^2\text{K}$, and $0.47 \text{ W/m}^2\text{K}$, respectively. In contrast, the Q1500, CPS, and W1 walls exhibit higher (and therefore less favorable) Y_{ie} values.

From Figure 11, it can be found that the time lag of the *quincha* walls is the highest, with Q500's at 6.97 h and Q1500's at 6.37 h. The time lag values of the other wall solutions

are all below 4 h: 2.20 h for wall W1, 3.69 h for wall W2, 3.90 h for the LSF wall, and 3.51 h for the CPS wall. Even though all the estimated time lag values are below 12 h, the *quincha* walls have the best performance, independently of the bulk density of the *quincha* mix.

Figure 12 shows that the decrement factors of the W1, W2, LSF, and CPS wall constructions are similar. The W1 wall has a decrement factor of 0.934, which improves to 0.870 with the addition of interior insulation (W2 wall). The LSF wall shows a decrement factor of 0.877, while the CPS system achieves 0.812. In comparison, the Q500 and Q1500 walls perform significantly better, with decrement factors of 0.600 and 0.523, respectively.

3.1.3. Roofs

In Figure 13, similarly to the previous observations for the wall solutions, the best U-value performance is found for the W2 roof system ($0.25 \text{ W/m}^2\text{K}$), followed by the LSF ($0.26 \text{ W/m}^2\text{K}$), Q500 ($0.61 \text{ W/m}^2\text{K}$), and CPS ($0.58 \text{ W/m}^2\text{K}$) roof systems. The W1 roof has the highest (and consequently the worst) U-value (equal to $3.01 \text{ W/m}^2\text{K}$), followed by the Q1500 roof (U-value equal to $1.26 \text{ W/m}^2\text{K}$).

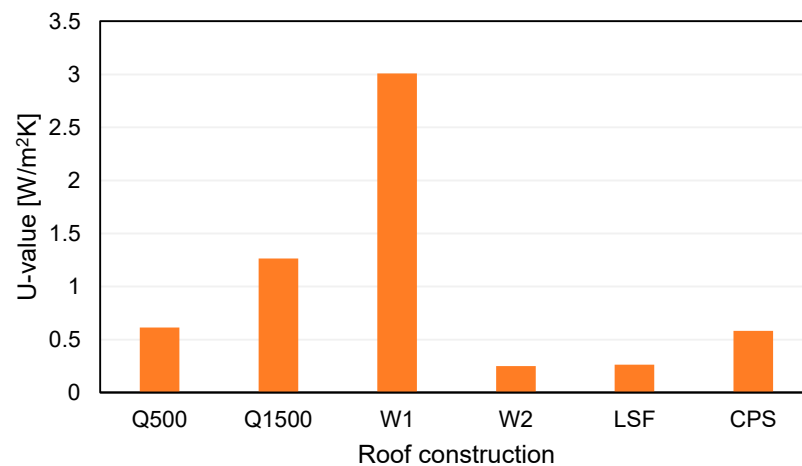


Figure 13. U-values of the investigated roof building systems.

Figure 14 demonstrates that using a higher-density earth mix significantly increases the surface mass of the Q1500 roof solution to 287.36 kg/m^2 . Other high-performing roof solutions include the CPS at 174.53 kg/m^2 , followed by Q500 at 137.36 kg/m^2 , the LSF at 104.46 kg/m^2 , and W2 at 94.3 kg/m^2 . The W1 roof, meanwhile, has a lower surface mass of 67.1 kg/m^2 .

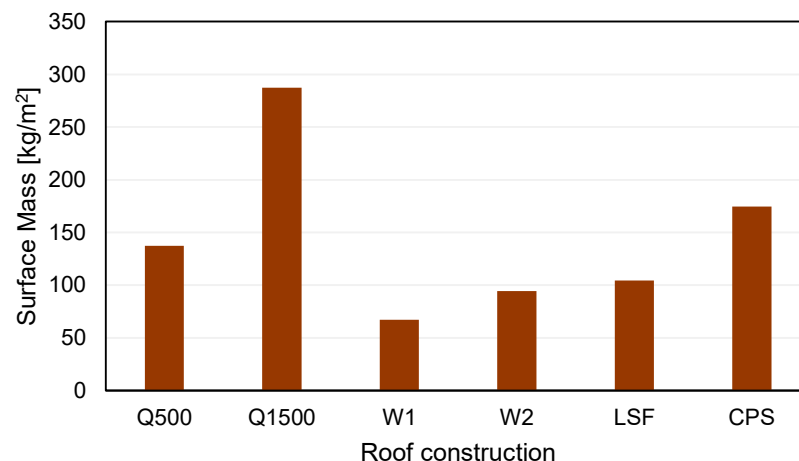


Figure 14. Surface masses of the investigated roof building systems.

Figure 15 shows the periodic thermal transmittance of the analyzed roof solutions. The W2 roof has the lowest (and so the best) Y_{ie} values ($0.21 \text{ W/m}^2\text{K}$). It is followed by the Q500 and LSF roofs' Y_{ie} values (both $0.24 \text{ W/m}^2\text{K}$) and those of the Q1500 roof ($0.29 \text{ W/m}^2\text{K}$) and CPS roof ($0.50 \text{ W/m}^2\text{K}$), while the W1 solution is the worst ($Y_{ie} = 2.99 \text{ W/m}^2\text{K}$).

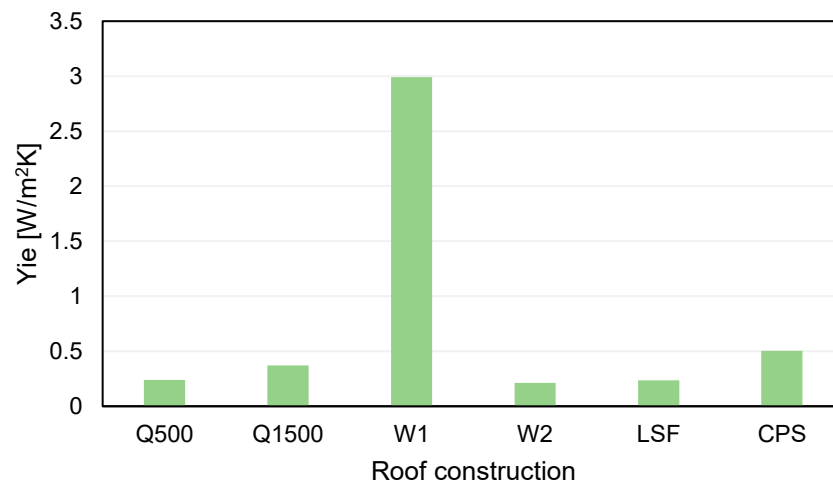


Figure 15. Periodic thermal transmittance of the investigated roof building systems.

In Figure 16, the time lag values of different roof constructions are shown. Both earth density values (used in the Q500 and Q1500 roof solutions) prove to efficiently delay the incoming heat flux to acceptable time lag values. Indeed, the time lag of the Q500 roof is the highest, at 9.48 h, followed by Q1500 (8.94 h), W2 (4.48 h), LSF (3.67 h), CPS (3.05 h), and W1 (0.63 h).

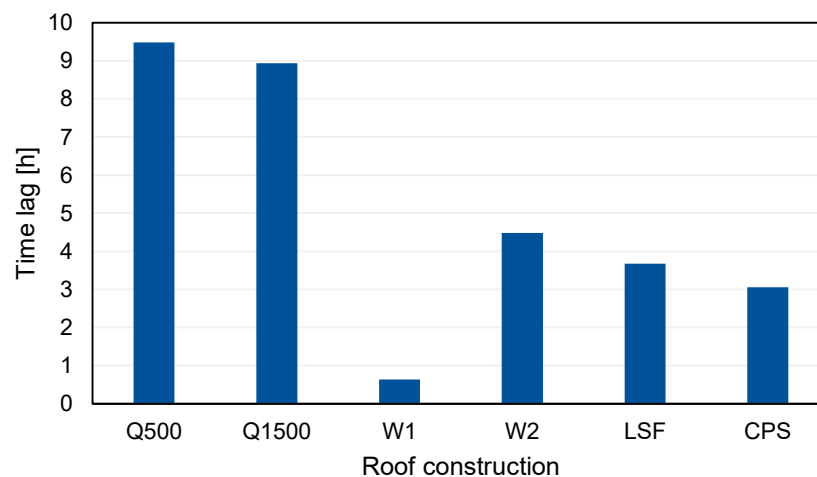


Figure 16. Time lags of the investigated roof building systems.

Both earth density values optimize the decrement factor value (see Figure 17). Indeed, for Q500, a DF value of 0.39 is found, while for Q1500, the DF value is 0.29. All the other roof solutions have DF values above 0.86. The relatively higher thermal mass of the earth mix used in *quincha* solutions reduces the decrement factor value, dampening outer heat transmission.

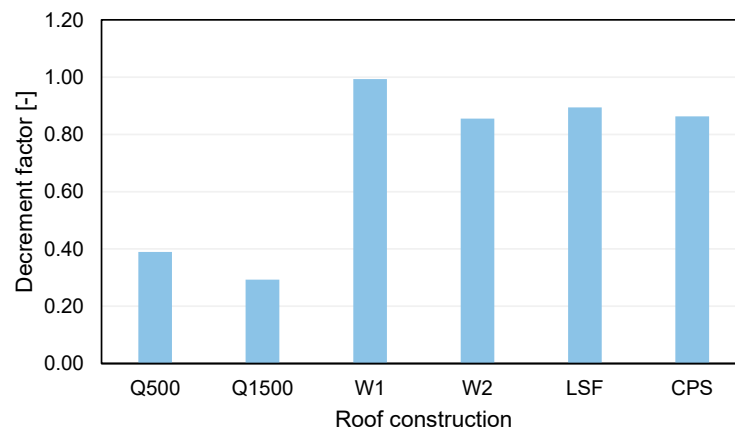


Figure 17. Decrement factors of the investigated roof building systems.

3.2. Environmental Performance Levels

Table 3 presents the results of the Life Cycle Assessment (LCA) for the analyzed systems, while Figures 18–21 report the details of the various phases' incidence in the different impact categories.

Table 3. Environmental impacts of the investigated systems.

System	Environmental Impacts			
	CF	Carbon Storage	WF	EE
	kgCO ₂ eq	kgCO ₂ eq	m ³	GJ
Q	2635.47	−5670.21	2303.07	42.70
W1	12,152.61	−4970.21	2141.09	148.01
W2	12,927.00	−4968.33	2466.00	158.40
LSF	14,142.00	−258.87	2640.00	150.40
CPS	17,338.58	-	6441.90	124.60

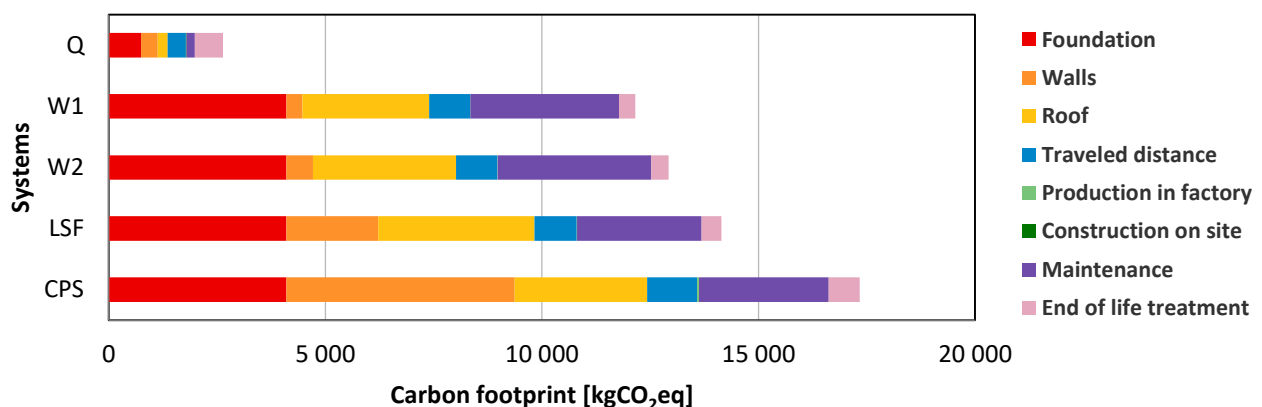


Figure 18. Carbon footprints of the investigated systems.

Figure 18 illustrates the carbon footprints (CFs) of the different building systems analyzed. The quincha system has the lowest CF at 2635.47 kgCO₂eq, minimized across all phases due to the use of locally sourced, low-processed materials (earth, straw, sand, stone). The upstream phase, particularly the foundation construction stage, exhibits the highest carbon footprint (CF) in this system. The W1 system has the second-lowest CF at 12,152.61 kgCO₂eq, though it is more than five times higher than that of the quincha system. In the W1 system, the upstream phase—primarily due to the concrete foundation and roof—contributes most significantly to the CF. Additionally, the maintenance phase

impacts the CF due to the assumed replacement of the corrugated metal roofing every 50 years. The W2 system’s CF is slightly higher than W1’s, at 12,927.00 kgCO₂eq, mainly due to the use of glass wool insulation in the walls and roof. The LSF system shows a higher CF at 14,142.00 kgCO₂eq, attributed to materials used in the walls during the upstream phase, particularly steel profiles, glass wool insulation, and cement plaster.

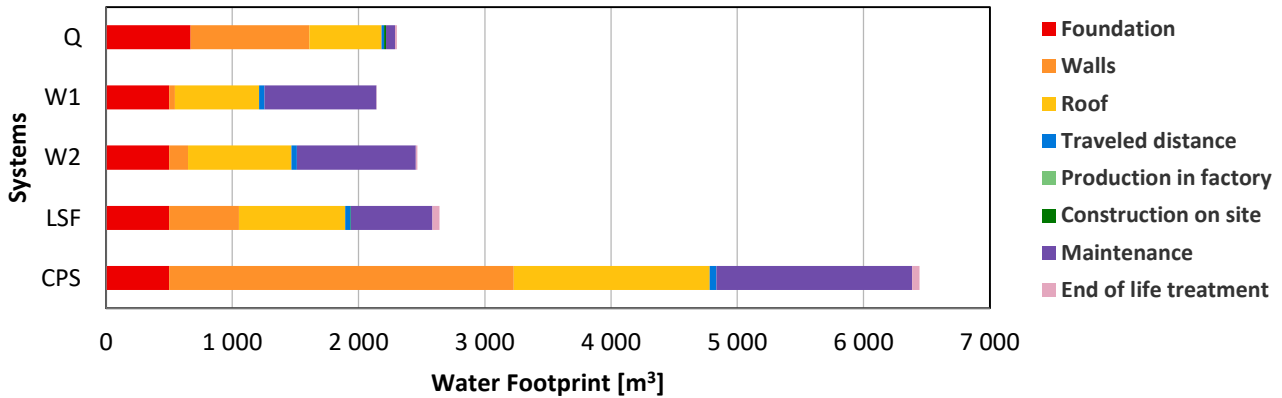


Figure 19. Water footprints of the investigated systems.

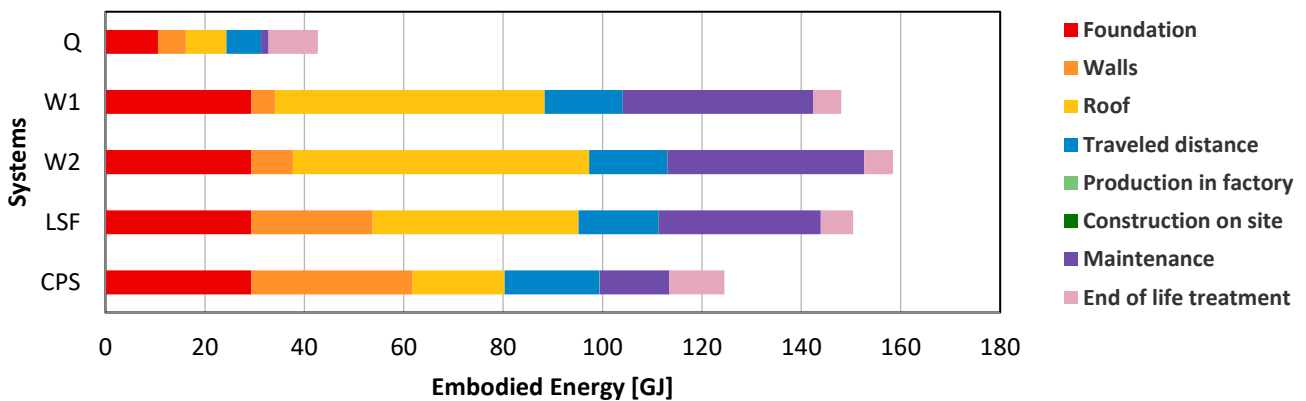


Figure 20. Embodied energies of the investigated systems.

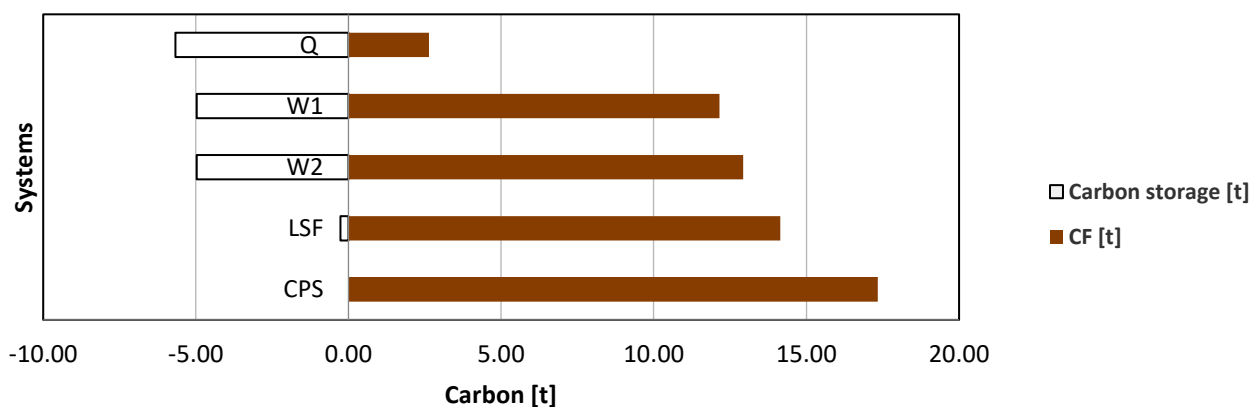


Figure 21. Carbon storage levels versus carbon footprints of the investigated systems.

Finally, the CPS system has the highest CF at 17,338.58 kgCO₂eq, driven largely by the high use of cement, EPS, and steel in the wall systems. Furthermore, the CF associated with transportation is elevated due to the need to transport heavy materials to the construction site.

Figure 19 presents the water footprint (WF) of the building systems analyzed. The W1 system has the lowest WF, amounting to 2141.09 m³, largely due to its prefabricated

timber structure, which employs a dry assembly method that significantly reduces water consumption. The primary contributors to the WF in this system are maintenance, particularly the periodic replacement of wood paint every 20 years, and the upstream phase, with roofing and foundation materials being the main sources of water use.

The Q system ranks as the second lowest in water footprint (WF), with a total of 2303.84 m³. However, it shows higher impacts during the upstream phase, primarily due to water usage in foundation and wall construction. In the *quincha* building system, water plays a vital role in facilitating both physical reactions (in earthen materials) and chemical reactions (in lime and cement), which are essential for forming strong bonds. The W2 system, with a WF of 2466.00 m³, exhibits higher impacts in the walls and roof sections, largely attributed to the use of glass wool insulation. The LSF system has a relatively high water footprint (WF) of 2640.00 m³, largely driven by the upstream phase due to the significant use of steel and glass wool insulation in the walls, as well as contributions from the end-of-life phase. In comparison, the CPS system exhibits the highest WF, totaling 6441.90 m³, primarily resulting from the extensive use of cement in both the wall and roof systems. Additionally, its maintenance WF is notably elevated due to the periodic replacement of cement mortar, which contributes substantially to its overall water consumption.

Figure 20 illustrates the embodied energy (EmE) results of the building systems analyzed. The Q system has the lowest EmE at 42.70 GJ, with the highest impacts associated with the materials used for the foundation. For the walls, this system uses local materials, which do not require energy-intensive processing, and minimal machinery in the constructive phase (only a mixer for preparing the mixture). The CPS system has an EmE of 124.60 GJ, nearly four times higher than the Q system, primarily due to the upstream phase, which involves energy-intensive materials for the foundations, walls, and roof, as well as the transportation of these materials to the site. The W1 and LSF systems have similar EmE values, at 148.02 GJ and 150.40 GJ, respectively. The LSF system's higher upstream impacts are related to the walls, while the W1 system has an increased EmE in both the upstream and maintenance phases, mainly due to the roofing. Lastly, the W2 system has the highest EmE, at 158.40 GJ, primarily due to the addition of glass wool insulation.

Figure 21 makes a comparison between the carbon storage capacity and the carbon footprint (CF) of the building systems analyzed. The Q system, which incorporates a significant amount of straw and timber during its upstream phase, achieves carbon storage levels that not only fully offset but also exceed its CF, highlighting its net-positive carbon performance. In contrast, the W1 and W2 systems demonstrate partial offsetting of their CFs through carbon storage. The LSF system, however, exhibits minimal carbon storage, making its offset negligible. Lastly, the CPS system, which does not include any natural materials, lacks carbon sequestration potential entirely, resulting in no offset of its CF.

3.3. Carbon Footprint Results: Comparison with the Literature

Since CO₂ emissions are the most commonly assessed category in the literature, the tiny house systems analyzed in this study are compared with similar buildings in terms of carbon footprint. However, to ensure consistency, the operational phase—typically the largest contributor to climate change impacts [21–23,25] and accounting for 70–80% of total CO₂ emissions due to heating, cooling, and electricity—is excluded from the comparison, as the case study in Chile lacks heating and cooling systems. In order to effectively compare the obtained results with those of previous studies, it is necessary to express the carbon footprint of the tiny house per square meter of floor area, which will serve as a new functional unit, useful for the comparison. Table 4 presents case studies from the literature, including the main building materials used, their floor area, the location, and the stages of LCA included in the analysis. The carbon footprint values, calculated based on

a square meter of floor area, highlight the significantly lower carbon footprint of the *quincha* construction system investigated in this work. This reduction is attributed to the use of local materials and labor-intensive methods with minimal machinery, in contrast to other systems that rely on energy-intensive processes and industrialized transformation of raw materials. It should be noted that comparing tiny houses in different climates remains challenging due to differences in thermal envelope performance requirements. Furthermore, it should be noted that not all the reported studies present the same LCA stages.

Table 4. Comparison of life cycle carbon footprints for the studied tiny houses and cases studies from the literature.

REF	Main Building Materials	m ²	Location	Stages	CF [kg CO ₂ eq/m ²]
This study	Q system (wood, earth, straw)	28	Chile	Upstream, Transport, Construction, Maintenance, End of Life	94.12
This study	W1 system (wood)	28	Chile	Upstream, Transport, Construction, Maintenance, End of Life	434.02
This study	W2 system (wood, stone wool)	28	Chile	Upstream, Transport, Construction, Maintenance, End of Life	461.69
This study	LSF system (steel, stone wool)	28	Chile	Upstream, Transport, Construction, Maintenance, End of Life	505.07
This study	CPS system (steel, EPS, concrete)	28	Chile	Upstream, Transport, Construction, Maintenance, End of Life	619.24
[15]	Wood, steel	12.2	Australia	Upstream, Transport, Construction, Maintenance, End of Life	418.85
[21]	Steel, concrete panels	18	United Arab Emirates	Upstream, Transport, Construction, Maintenance, End of Life	2640.00
[23]	Wood (CLT), metal sheet slate	16	Finland	Upstream, Transport, Construction, Maintenance, End of Life	486.50
[24]	Steel	56	Portugal	Upstream, Transport, Construction	375.00
[24]	Concrete	56	Portugal	Upstream, Transport, Construction	482.14
[24]	Timber	56	Portugal	Upstream, Transport, Construction	303.57
[24]	LSF	56	Portugal	Upstream, Transport, Construction	312.50
[25]	PVC, PU, PVC, rockwool, plasterboard	56	Portugal	Upstream, Transport, Construction	625.00

3.4. Comparison of Thermal and Environmental Performance Levels

Figure 22 shows a radar graph containing the analyzed systems' thermal and environmental performance levels. For the sake of brevity, the reported thermal performance levels refer to the U-value and to the surface mass of walls and roof systems. A normalization criterion is applied to the following graph: the values have been normalized to the best performances so that a value near the center of the graph is a worse performance compared to a value near the vertexes of the graph, representing the best performance.

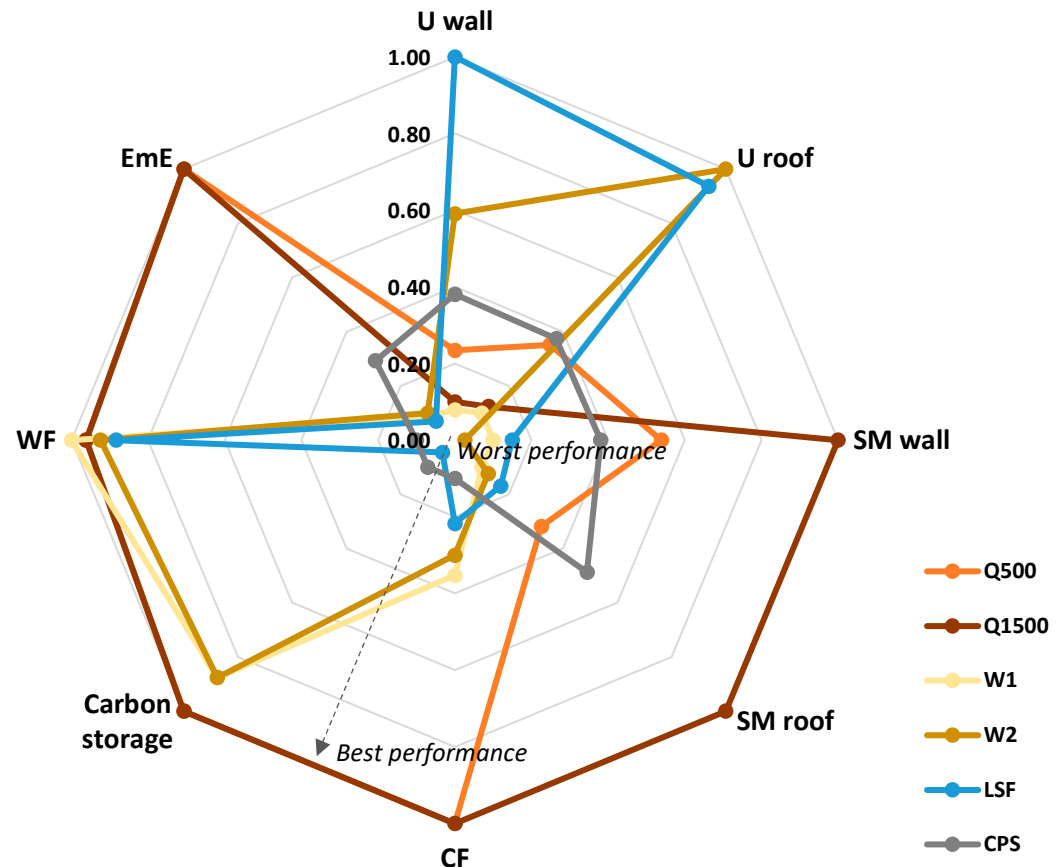


Figure 22. Radar graph for performance comparison between the analyzed systems.

As it can be appreciated from the radar graph, the *quincha* system has the best environmental performance, with a low CF, high carbon storage, and low EmE, though its WF is slightly higher than the W1 system. The thermal performance of the *quincha* wall varies with density: maintaining a density of 500 kg/m^3 ensures good yet not excellent thermal insulation, while increasing it to 1500 kg/m^3 reduces thermal insulation; on the other hand, the surface mass of the *quincha* wall is lower in the Q500 scenario compared to the Q1500 one (which has the highest absolute surface mass). The LSF system has good thermal insulation properties but high environmental impacts, mainly because it uses highly energy-intensive materials and processes. Similar considerations can be made for the CPS system, which has both low thermal and environmental performance levels. The worst thermal and environmental performance levels are those of the W1 system, which nonetheless has the lowest WF. W2, which represents an improvement on the W1 system, manages to improve the thermal performance of the W1 system at the expense of the CF, WF, and EmE, which all increase.

4. Conclusions

This study underscores the substantial environmental benefits of utilizing *quincha*—a traditional building technique that incorporates natural and locally sourced materials—for the construction of sustainable housing, exemplified by the tiny house in Chile’s Elqui Valley. Through a Life Cycle Assessment approach, the research reveals that the *quincha* construction method significantly reduces the carbon footprint compared to conventional construction techniques that rely on synthetic or industrial materials. In particular, the following findings have been presented:

- The carbon footprint (CF) of the *quincha* system is the lowest in absolute terms at 2635.47 kgCO₂eq. The second-lowest CF belongs to the wooden prefabricated system W1, at 12,152.61 kgCO₂eq, while the highest is that of the Concrete Panel System with EPS insulation (CPS), at 17,338.58 kgCO₂eq. The *quincha* system reduces the carbon footprint by up to 85% compared to the other systems using synthetic or industrial materials.
- The water footprint (WF) of the W1 system is the lowest in absolute terms at 2141.09 m³. The second-lowest WF belongs to the Q system (2303.07 m³), while the highest is that of the CPS system, at 6441.90 m³. Compared to systems using concrete and EPS panels (CPS), the *quincha* system reduces the water footprint by up to 64%.
- The embodied energy (EE) of the *quincha* system is the lowest in absolute terms at 42.70 GJ. The second-lowest EE belongs to the CPS system, at 124.60 GJ, while the highest in absolute terms is that of the wooden prefabricated system with glass wool insulation (W2), at 158.40 GJ. The *quincha* system reduces the embodied energy by up to 73% compared to the other prefabricated systems.
- Due to the high amount of wood and straw involved in its construction, the carbon storage of the *quincha* system is −5670.21 kgCO₂eq, making it the only system that can compensate, theoretically, for its carbon footprint, thus reaching carbon neutrality. The wooden prefabricated systems W1 and W2 present carbon sequestration potential (at −4970.21 kgCO₂eq and −4968.33 kgCO₂eq, respectively), but not enough to compensate for their CFs.

Moreover, the thermal performance of key building components—foundations, walls, and roof systems—has been assessed, highlighting their role in enhancing the expected energy performance. In this regard, it is possible to state the following:

- The systems that provide the best thermal insulation are the LSF ($U_{\text{wall,roof}} = 0.26 \text{ W/m}^2\text{K}$) and W2 ($U_{\text{wall}} = 0.41 \text{ W/m}^2\text{K}$, $U_{\text{roof}} = 0.25 \text{ W/m}^2\text{K}$) systems, while both the *quincha* ($U_{\text{wall}} = 0.79 \text{ W/m}^2\text{K}$, $U_{\text{roof}} = 0.61 \text{ W/m}^2\text{K}$) and CPS ($U_{\text{wall}} = 0.57 \text{ W/m}^2\text{K}$, $U_{\text{roof}} = 0.58 \text{ W/m}^2\text{K}$) systems have higher U-values.
- The systems with higher surface mass are the *quincha* system Q500 ($SM_{\text{wall}} = 186.00 \text{ kg/m}^2$, $SM_{\text{roof}} = 137.36 \text{ kg/m}^2$) and the CPS system ($SM_{\text{wall}} = 137.93 \text{ kg/m}^2$, $SM_{\text{roof}} = 174.53 \text{ kg/m}^2$), while the lightweight prefabricated systems (W1, W2, and LSF) have lower SM values.
- The expected time lag and decrement factor of the *quincha* system Q500 walls ($DF = 6.97 \text{ h}$ and $TL = 0.60$, respectively) are better than the corresponding values for all the lightweight prefabricated systems (W1, W2, and LSF) and even for the medium-weight CPS system, which all have TL values below 4 h and DF values higher than 0.81.

Although it has lower thermal insulation, *quincha*’s expected dynamic thermal performance is optimal for territories characterized by large temperature shifts, such as the Elqui Valley, where lightweight prefabricated systems would suffer.

In light of these findings, some recommendations can be offered:

- Prioritizing locally sourced and natural materials can significantly reduce the environmental impact of construction while supporting local economies.
- Incorporating traditional building techniques like *quincha* can enhance thermal performance and provide sustainable alternatives to modern construction practices.
- Implementing Life Cycle Assessment (LCA) during the design process facilitates the identification of strategies to reduce environmental impacts, hence promoting sustainability throughout the building's life cycle.

Future research, including dynamic hygrothermal simulations, could provide deeper insights into how natural materials improve indoor comfort and overall building performance. Furthermore, a rigorous cost–benefit analysis could provide a more comprehensive framework, allowing the identification of the optimal solution in terms of total building cost.

Through Life Cycle Assessment (LCA), this study quantifies these environmental advantages, showcasing the potential for traditional building systems to align with modern sustainability objectives. The applied methodology facilitates a comprehensive evaluation of the building's environmental impact, creating a strong foundation for identifying further opportunities to enhance the sustainability of such constructions. Additionally, this research underscores the value of incorporating LCA during the design phase, as it yields actionable insights that may guide design modifications aimed at reducing environmental impacts.

Ultimately, this study provides compelling evidence of the environmental advantages of integrating traditional building techniques and natural materials into contemporary architecture. In addition to a reduced carbon footprint, these practices also show lower water footprint and embodied energy values, contributing to improving sustainability and resilience, particularly in regions like Chile's Elqui Valley, where resources are constrained and climate conditions are becoming increasingly unpredictable. By bridging traditional knowledge and modern sustainability practices, this approach offers a pathway to sustainable and adaptive building solutions.

Author Contributions: Conceptualization, G.G., L.D., N.J.S., R.M.P. and R.C.; methodology, G.G., L.D., N.J.S., R.M.P. and R.C.; software, R.M.P.; validation, L.D. and R.M.P.; formal analysis, G.G., L.D. and R.M.P.; investigation, G.G., L.D. and R.M.P.; resources, L.D., N.J.S., R.M.P. and R.C.; data curation, L.D. and G.G.; writing—original draft preparation, L.D. and G.G.; writing—review and editing, G.G., L.D., N.J.S., R.M.P. and R.C.; visualization, G.G. and L.D.; supervision, L.D., N.J.S., R.M.P. and R.C.; project administration, L.D., N.J.S., R.M.P. and R.C.; funding acquisition, L.D., N.J.S., R.M.P. and R.C. All authors have read and agreed to the published version of the manuscript.

Funding: This research received no external funding.

Data Availability Statement: Dataset available on request from the authors.

Acknowledgments: The authors would like to acknowledge Laura Mannucci for her graphical work on the tiny house technical drawings.

Conflicts of Interest: The authors declare no conflicts of interest.

References

1. United Nations Environment Programme; Yale Center for Ecosystems + Architecture. Building Materials and the Climate: Constructing a New Future. Available online: <https://wedocs.unep.org/20.500.11822/43293> (accessed on 6 December 2024).
2. Meadows, D.H.; Meadows, D.L.; Randers, J.; Behrens, W.W. *The Limits to Growth*; Universe Books: New York, NY, USA, 1972.
3. Park, S.; Cho, K.; Choi, M. A Sustainability Evaluation of Buildings: A Review on Sustainability Factors to Move towards a Greener City Environment. *Buildings* **2024**, *14*, 446. [[CrossRef](#)]
4. Akbarnezhad, A.; Xiao, J. Estimation and minimization of embodied carbon of buildings: A review. *Buildings* **2017**, *7*, 5. [[CrossRef](#)]
5. Chen, Z.; Chen, L.; Zhou, X.; Huang, L.; Sandanayake, M.; Yap, P.-S. Recent Technological Advancements in BIM and LCA Integration for Sustainable Construction: A Review. *Sustainability* **2024**, *16*, 1340. [[CrossRef](#)]

6. Eichner, M.J.; Elsharawy, H.H. Life Cycle Assessment (LCA) Based Concept Design Method for Potential Zero Emission Residential Building. *IOP Conf. Ser. Earth Environ. Sci.* **2020**, *410*, 012031. [CrossRef]
7. Faludi, J.; Lepech, M.D.; Loisos, G. Using life cycle assessment methods to guide architectural decision-making for sustainable prefabricated modular buildings. *J. Green Build.* **2012**, *7*, 151–170. [CrossRef]
8. Arowoia, V.A.; Onososen, A.O.; Moehler, R.C.; Fang, Y. Influence of Thermal Comfort on Energy Consumption for Building Occupants: The Current State of the Art. *Buildings* **2024**, *14*, 1310. [CrossRef]
9. Giuffrida, G.; Detommaso, M.; Nocera, F.; Caponetto, R. Design optimisation strategies for solid rammed earth walls in Mediterranean climates. *Energies* **2021**, *14*, 325. [CrossRef]
10. Minke, G. *Building with Earth: Design and Technology of a Sustainable Architecture*; Birkhäuser: Berlin, Germany, 2006.
11. Guillaud, H.; Houben, H.; CRAterre; Dethier, J. *Traité de Construction en Terre*; Parenthèses Editions: Marseille, France, 2006.
12. Marcom, A. *Construire en Terre-Paille*; Terre Vivante: Mens, France, 2011.
13. Acevedo, R.; Carrillo, O.; Broughton, J. *Construcción en Quincha Liviana: Sistemas Constructivos Sustentables de Reinterpretación Patrimonial*; Publication resulting from research funded by the Depto de Estudios, División Técnica de Estudios y Fomento Habitacional (DITEC) del Ministerio de Vivienda y Urbanismo y Fondart Nacional; Ministerio de Vivienda y Urbanismo y Fondart Nacional: Santiago, Chile, 2017.
14. Fiebig-Wittmaack, M.; Pérez, C.V.; Lazo, E.B. Aspectos climaticos del Valle del Elqui. In *Los Sistemas Naturales de la Cuenca del Río Elqui (Región de Coquimbo, Chile): Vulnerabilidad y Cambio del Clima*; Cepeda, P.J., Ed.; Ediciones Universidad de La Serena: La Serena, Chile, 2008; pp. 41–62.
15. Crawford, R.H.; Stephan, A. Tiny House, Tiny Footprint? The Potential for Tiny Houses to Reduce Residential Greenhouse Gas Emissions. *IOP Conf. Ser. Earth Environ. Sci.* **2020**, *588*, 022073. [CrossRef]
16. Chang, A. Evaluating Tiny Houses as a Solution to the Housing Affordability and Environmental Crises. *Aleth. Arts Sci. Acad. J.* **2023**, *3*, 11–15. [CrossRef]
17. Ford, J.; Gomez-Lanier, L. Are Tiny Homes Here to Stay? A Review of Literature on the Tiny House Movement. *Fam. Consum. Sci. Res. J.* **2017**, *45*, 394–405. [CrossRef]
18. Saxton, M.W. *Environmental Impacts of Tiny Home Downsizers: A Call for Research*; Research Monograph Series; Virginia Polytechnic Institute and State University: Blacksburg, VA, USA, 2019; Chapter 2; pp. 16–29.
19. Hooper, N.; Moreno-Beals, M. Pathways for Lifecycle Building Practices: Material Reuse in Tiny Home Construction, Co-Learning Plan—2019 Michigan State University. Available online: https://reicenter.org/upload/documents/colearning/tiny-houses_web.pdf (accessed on 6 December 2024).
20. Mukhopadhyay, J. Observations of Energy Consumption and IEQ in a ‘Tiny House’. *Build. Res. Inf.* **2020**, *48*, 613–631. [CrossRef]
21. Sabobeh, L.; Al Hassani, R.; Alomar, L.; Atabay, S.; Mortula, M.M.; Ali, T.A.; Taher, A.M. Life cycle assessment of the tiny house initiative in the United Arab Emirates. *Front. Sustain. Cities* **2024**, *6*, 1488269. [CrossRef]
22. Ruiz-Pastor, L.; Altavilla, S.; Nezzi, C.; Borgianni, Y.; Orzes, G. Life Cycle Assessment of a Mobile Tiny House Made with Sustainable Materials and Design Implications. In *Advances on Mechanics, Design Engineering and Manufacturing IV, Proceedings of the International Joint Conference on Mechanics, Design Engineering & Advanced Manufacturing, JCM 2022, 1–3 June 2022, Ischia, Italy*; Gerbino, S., Lanzotti, A., Martorelli, M., Mirálbes Buil, R., Rizzi, C., Roucoules, L., Eds.; Lecture Notes in Mechanical Engineering; Springer: Cham, Switzerland, 2023. [CrossRef]
23. Kuittinen, M.; Ruuska, K.; Viriyaraj, B.; Zubillaga, L. Are ‘tiny homes’ good for the environment? Focus on materials, land-use, energy and carbon footprint. *J. Archit.* **2023**, *28*, 698–722. [CrossRef]
24. Tavares, V.; Lacerda, N.; Freire, F. Embodied energy and greenhouse gas emissions analysis of a prefabricated modular house: The “Moby” case study. *J. Clean. Prod.* **2019**, *212*, 1044–1053. [CrossRef]
25. Tavares, V.; Freire, F. Life cycle assessment of a prefabricated house for seven locations in different climates. *J. Build. Eng.* **2022**, *53*, 104504. [CrossRef]
26. Ben-Alon, L.; Loftness, V.; Harries, K.A.; Cochran Hameen, E. Life Cycle Assessment (LCA) of Natural vs. Conventional Building Assemblies. *Renew. Sustain. Energy Rev.* **2021**, *144*, 110951. [CrossRef]
27. Mateus, R.; Fernandes, J.E.P.; Teixeira, E.R. Environmental Life Cycle Analysis of Earthen Building Material. In *Encyclopedia of Renewable and Sustainable Materials*; Elsevier Inc.: Amsterdam, The Netherlands, 2019. [CrossRef]
28. Arduin, D.; Caldas, L.R.; Paiva, R.d.L.M.; Rocha, F. Life Cycle Assessment (LCA) in Earth Construction: A Systematic Literature Review Considering Five Construction Techniques. *Sustainability* **2022**, *14*, 13228. [CrossRef]
29. Melià, P.; Ruggieri, G.; Sabbadini, S.; Dotelli, G. Environmental impacts of natural and conventional building materials: A case study on earth plasters. *J. Clean. Prod.* **2014**, *80*, 179–186. [CrossRef]
30. Cabeza, L.F.; Barreneche, C.; Miró, L.; Morera, J.M.; Bartolí, E.; Fernandez, A.I. Low carbon and low embodied energy materials in buildings: A review. *Renew. Sustain. Energy Rev.* **2013**, *23*, 536–542. [CrossRef]
31. Narayanaswamy, A.H.; Walker, P.; Reddy, B.V.V.; Heath, A.; Maskell, D. Mechanical and thermal properties, and comparative life-cycle impacts of stabilised earth building products. *Constr. Build. Mater.* **2020**, *243*, 118096. [CrossRef]

32. Prudente, L.T. Life-Cycle Assessment of the Environmental Impact of Earthen Buildings versus Conventional Buildings on Human Health. In *Sustainability and Toxicity of Building Materials*; Petrović, E.K., Gjerde, M., Chicca, F., Marriage, G., Eds.; Woodhead Publishing Series in Civil and Structural Engineering; Woodhead Publishing: Sawston, UK, 2024; pp. 289–306. [[CrossRef](#)]
33. Caldas, R.L.; de Lima Moura Paiva, R.; Paiva de Souza Martins, A.; Dias Toledo Filho, R. Argamassas de terra versus convencionais: Avaliação do desempenho ambiental considerando o ciclo de vida. *MIX Sustent.* **2020**, *6*, 115–128. [[CrossRef](#)]
34. Curth, A.; Pearl, N.; Castro-Salazar, A.; Mueller, C.; Sass, L. 3D printing earth: Local, circular material processing, fabrication methods, and Life Cycle Assessment. *Constr. Build. Mater.* **2024**, *421*, 135714. [[CrossRef](#)]
35. Dipasquale, L.; Ammendola, J.; Montoni, L.; Ferrari, E.P.; Zambelli, M. Harnessing Vernacular Knowledge for Contemporary Sustainable Design through a Collaborative Digital Platform. *Heritage* **2024**, *7*, 5251–5267. [[CrossRef](#)]
36. Ojeda, V.; Vega-Jorquera, P.; De La Barra, E.; Palma-Chilla, L.; Vidal, L.; Saavedra, J.; Pizarro, A. Characterization of Seismicity and Seismic Hazard in the Coquimbo Region, Chile: A Probabilistic Study. *Pure Appl. Geophys.* **2024**, *181*, 1427–1454. [[CrossRef](#)]
37. The World Bank. La Construcción de Viviendas en Madera en Chile: Un Pilar para el Desarrollo Sostenible y la Agenda de Reactivación. 2020. Available online: <https://documents1.worldbank.org/curated/en/224671607109191179/pdf/The-Construction-of-Timber-Houses-in-Chile-A-Pillar-of-Sustainable-Development-and-the-Agenda-for-Economic-Recovery.pdf> (accessed on 6 December 2024).
38. Ramírez, C.F.; Casares, M. Sistemas constructivos no tradicionales. Modelos para armar. *BIT* **2011**, *79*, 14–23.
39. Convitec. Manual Técnico. Available online: <https://sjnavarro.wordpress.com/wp-content/uploads/2008/08/manual-tecnico-covintec-2011.pdf> (accessed on 6 December 2024).
40. *ISO 10456:2007*; Building Materials and Products—Hygrothermal Properties—Tabulated Design Values and Procedures for Determining Declared and Design Thermal Values. International Standard Organization: Geneva, Switzerland, 2023.
41. Giuffrida, G.; Dipasquale, L.; Pulselli, R.M.; Caponetto, R. Compared Environmental Lifecycle Performances of Earth-Based Walls to Drive Building Envelope Design. *Sustainability* **2024**, *16*, 1367. [[CrossRef](#)]
42. Giuffrida, G.; Caponetto, R.; Nocera, F. Hygrothermal Properties of Raw Earth Materials: A Literature Review. *Sustainability* **2019**, *11*, 5342. [[CrossRef](#)]
43. Volhard, F. *Light Earth Building: A Handbook for Building with Wood and Earth*, 1st ed.; Birkhäuser: Basel, Switzerland, 2016.
44. Wieser, M.F.; Onnis, S.; Meli, G. Conductividad Térmica de la Tierra Alivianada con Fibras Naturales en Paneles de Quincha. En Seminario Iberoamericano de Arquitectura y Construcción con Tierra. SIACOT 2018 Red Iberoamericana de Arquitectura y Construcción con Tierra. pp. 199–208. Available online: <http://siacot.ingenieria.usac.edu.gt/index.php/memorias> (accessed on 6 December 2024).
45. *ISO 13786:2018*; Thermal Performance of Building Components—Dynamic Thermal Characteristics—Calculation Methods. International Standard Organization: Geneva, Switzerland, 2018.
46. Taylor, T.J. The role of thermal mass in low-slope roof design. International Institute of Building Enclosure Consultants. *IIBEC Interface* **2022**, 26–31. Available online: <https://iibec.org/wp-content/uploads/2022-01-taylor.pdf> (accessed on 6 December 2024).
47. Ulgen, K. Experimental and theoretical investigation of effects of wall's thermophysical properties on time lag and decrement factor. *Energy Build.* **2002**, *34*, 273–280. [[CrossRef](#)]
48. *ISO 14040:2006*; Environmental Management. Life Cycle Assessment: Principles and Framework. International Standard Organization: Geneva, Switzerland, 2006.
49. *UNI EN ISO 14044:2020*; Gestione Ambientale-Valutazione del Ciclo di Vita-Requisiti e Linee Guida. International Standard Organization: Geneva, Switzerland, 2020.

Disclaimer/Publisher's Note: The statements, opinions and data contained in all publications are solely those of the individual author(s) and contributor(s) and not of MDPI and/or the editor(s). MDPI and/or the editor(s) disclaim responsibility for any injury to people or property resulting from any ideas, methods, instructions or products referred to in the content.